

Cavity noise generation for circular and rectangular vent holes

Michael J Czech^{*}, Jeffrey D Crouch[†] and Robert W Stoker[‡]
The Boeing Company, Renton, WA

Michael Kh.. Strelets[§]
“New Technologies and Services” (NTS), St.-Petersburg, Russia

and

Andrey Gabaruk[¶]
St.-Petersburg State Polytechnic University, St.-Petersburg, Russia

Flight tests on a Boeing 777 showed the occurrence of a tone generated by circular anti-icing vents on the underside of a slat during approach conditions. Subsequent wind-tunnel tests are conducted with a full-scale 4ft-span section of the slat at Mach numbers ranging from 0.1 to 0.3. The objective of the wind-tunnel tests is to replicate and then alleviate the tone. Six different vent openings are tested including rectangular and circular shapes constrained by maintaining the overall open area of the vents. Tones are observed at a Strouhal number around 0.4 for the different vent geometries, based on the free-stream velocity and the effective streamwise length of the vent opening. The experimental results also show a sudden tone cut-off as the Mach number is increased; the critical Mach number being dependent on the cavity length.

A two-dimensional model of the cavity is developed to enable numerical simulation of the flow. The geometric length scales and Mach numbers are chosen to expand on the experiment findings, but the unknown experimental momentum thickness has to be estimated. The numerical simulations are based on a laminar inflow boundary layer with the initial momentum thickness as a variable. General features of the numerical simulations are in good agreement with the experiments. The simulations show tone cut-on at conditions similar to observations on simple cavity geometries. The tone cut-off with increasing Mach number is observed, but the conditions for its occurrence are not clearly defined.

I. Introduction

AIRFRAME noise arises mainly from the landing gear, and the slat and flap systems. Less frequently, tones may be generated by flow over pin holes, tube openings or cavities of various kinds. During the 2001 Quiet Technology Demonstrator program, a 2kHz tone was detected and localized on a Boeing 777-200 using a ground-based phased array system. Figure 1 illustrates phased-array noise contours at a frequency of 2kHz overlaid on a 777. The tone was generated at approach conditions and arose from circular anti-icing vent holes on the pressure side of the slat. These openings vent hot air, which circulates in the slat to prevent ice build-up. Removal of the tone through temporarily taping over the vent holes was determined to lead to a measurable reduction of the 777 approach noise levels. Figure 2 shows a simplified drawing of the slat geometry where the vent opening is backed by a large volume limiting fluid dynamic interactions between the cavity volume and the cavity shear layer.

^{*} Scientist/Engineer, Fluid Mechanics and Acoustics, 67-ML, AIAA Member

[†] Technical Fellow, Fluid Mechanics and Acoustics, 67-ML, AIAA Member

[‡] Scientist/Engineer, Fluid Mechanics and Acoustics, 67-ML, AIAA Member

[§] Principal Scientist

[¶] Associate Professor, Department of Aerodynamics and Thermodynamics

The flow-noise generation mechanism associated with vent holes may be considered similar to the classical cavity-noise source referred to as shear-layer mode oscillations or fluid-dynamic oscillations. This is distinct from fluid-resonant oscillations, where the frequency selection is essentially a function of the cavity geometry and examples would be organ pipes or side branches (Rockwell and Naudascher¹). The shear-layer induced noise results from an acoustic resonance, which is characterized by four elements. Disturbances in the free shear layer spanning the cavity are subject to Kelvin-Helmholtz instabilities and are amplified as they convect downstream. Upon impingement on the downstream edge of the cavity an acoustic field is generated. The acoustic pressure fluctuations propagate upstream across the cavity and excite the instabilities at the separation region creating a feedback loop. The feedback or upstream influence is essentially instantaneous for 'incompressible' flow while an acoustic delay has to be considered for higher Mach number flows.

An alternative oscillatory cavity mode, sometimes referred to as wake-mode oscillations (Gharib and Roshko²) may also exist for cavities with large dimensions relative to the boundary layer thickness. The cavity flow appears similar to a bluff-body wake flow and is, therefore, accompanied by a large drag increase. The oscillations in cavities exhibiting wake mode are sustained by recirculating flows in the cavity rather than by an acoustic feedback (Rowley et al³). The study of Rowley et al³ also postulated that transition to wake mode occurs if the Reynolds or Mach number are increased for a fixed cavity geometry. Reviews on cavity flows with focus on experimental and analytical work are given by Rockwell and Naudascher¹ and Blake and Powell⁴. A recent review paper by Colonius⁵ highlights numerical investigations of cavity flows, and active control strategies.

The governing parameters describing cavity oscillations are both plentiful and not well understood due to the coupling between the shear-layer dynamics and the cavity geometry. Most studies of cavity acoustics consider a open cavity characterized by a rectangular section of a given length and depth. The cavity length relative to the boundary-layer momentum thickness, the cavity length relative to the depth, and the Mach number are all known to have a strong influence on the cavity acoustics. Rossiter⁶ performed wind tunnel tests at subsonic and transonic Mach numbers investigating rectangular shallow cavities with streamwise length to depth ratios of 1 to 10. Based on the assumption of a feedback cycle, he proposed a semi-empirical expression describing the Strouhal number for these multi-stage feedback modes. A recent theoretical study on subsonic cavity flows by Kerschen and Tumin⁷ resulted in an expression of similar form as the Rossiter⁶ equation without the empirical constants. The cavity shear layer was approximated by a vortex sheet in the edge-scattering analyses to accommodate the main features of the oscillations.

While the Rossiter⁶ model proves to be very useful in determining the potential oscillatory modes of a cavity it gives no indication if these modes will occur or not. Observations and results towards an understanding of the occurrence of tones in flows over cavities were made by Sarohia⁸ in his study of laminar flow over shallow axisymmetric cavities. Sarohia⁸ noted that cavity oscillations would not occur below a given length at fixed flow conditions.

The current work investigates subsonic flow over vents with rectangular and circular openings. Experiments are conducted to model the baseline airplane vent configuration, as well as alternative configurations in order to alleviate the observed tone. The various vent-hole geometries are parameterized, and their aeroacoustic characteristics are related to simple-cavity noise. A numerical-simulation study is then conducted to further investigate the occurrence of tone cut on and cut off.

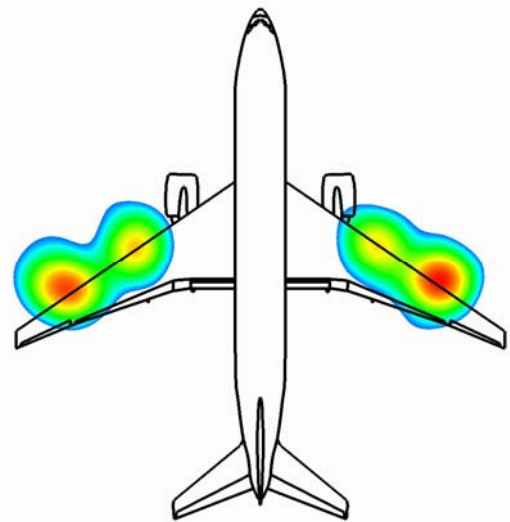


Figure 1. Acoustic map for a 777 at approach at 2kHz showing leading edge noise source.

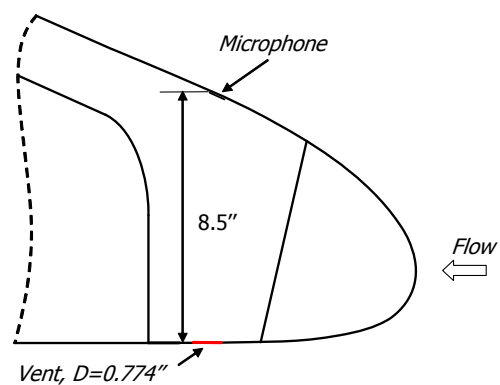


Figure 2. Schematic of a 777-slat geometry with vent opening.

II. Experimental study

A. Wind-tunnel test setup

Tests are conducted in two separate wind-tunnel facilities using the same model – a 4ft long section of a full-scale 777 leading-edge slat. The model is constructed to resemble the pressure distribution over a production slat attached to the main wing.

Initial testing in the Boeing Propulsion Wind Tunnel (9x9) is focused on replicating flight test results and gaining an understanding of the underlying tone mechanism. This solid-wall open-circuit facility has a cross-section of 9x9ft and a working-section length of 24ft. Air is drawn in through a bell mouth containing flow straightening and noise reduction vanes as well as screens for turbulence reduction. Free-stream turbulence intensity levels are about 0.25% over the band 3Hz to 10kHz. The blade-passage tone frequency ranges from 50 to 68Hz depending on power setting. Figure 3 shows a photograph of the slat model installed in the 9x9 facility mounted into a custom built fixture where a turn table allows angle of attack variations.

The second stage of the testing is conducted in the Boeing Research Aero-Icing Tunnel (BRAIT). This facility has a 4x6ft working section and the same 4ft slat section was used. Figure 4 is a photograph of the model installation in the BRAIT. A new baseline skin for the slat is built for this test with a replaceable plate in an area covering the six center anti-icing vent holes. A number of plates were designed and built with different hole geometries to investigate the influence of the vent shape on the tone amplitude and its occurrence.

Five microphones were installed within the slat-model to record the acoustic pressure field. The data signals were band-passed from 2Hz to 5kHz and recorded on tape. Calibration was performed prior to the test to ensure good signal to noise ratio and to obtain correct sensitivities. Pressure taps were installed on the external slat surfaces along the lip to obtain an understanding of the approaching boundary layer. The model blockage effects were accounted for in the determination of the free-stream velocities.

No boundary-layer characteristics were measured during the experiments. To estimate the incoming boundary-layer thickness for the simulations, laminar boundary-layer calculations are carried out using the slat c_p distributions at the wind-tunnel Reynolds numbers. The local momentum thickness for a laminar boundary layer is estimated to be approximately $\theta=0.004$ in. Boundary-layer stability calculations are done to determine if the boundary layer at the slot location is likely to be laminar or turbulent. The stability results suggest that the boundary layer at the slot is likely to be turbulent, but that some portion of the upstream boundary layer could be laminar. The fully turbulent boundary-layer momentum thickness is estimated to be around $\theta=0.014$ in.

B. Standard vent-hole results

The first experiments are conducted over a Mach number range from 0.1 to 0.275. The standard anti-icing vent holes are spaced 2.88in apart and have a diameter of 0.774in. These tests verify that the tones observed during flight can be reproduced and measured in the non-acoustically treated wind tunnel. Figure 5 shows results at a 3.1Hz



Figure 3. Slat model installed in the 9x9ft. Wind Tunnel.



Figure 4. Slat model installed in the BRAIT.

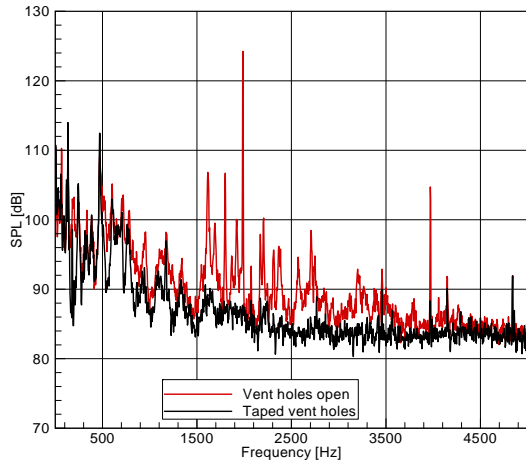


Figure 5. Anti-icing vent tones reproduced in the Boeing 9x9ft wind-tunnel (M=0.25)

bandwidth from the microphone installed in the slat volume at the wall opposite the vent opening. The transducer spectral density noise floor was at about 85dB providing the overall noise floor in the frequency region of interest from about 500Hz to 5kHz. A distinct tone of 124dB magnitude is found at a frequency of 2kHz for a Mach number of 0.25 and this is in very good agreement with the flight test results. A subsequent taping of all holes illustrates the good signal to noise ratio in the frequency region of interest. The taping further confirms the vent opening as the source of the observed tone and demonstrates the absence of facility-related high excitation levels close to the vent-hole tone frequency.

Given the ability to reproduce the observed flight-test results in the wind tunnel, further tests are conducted to gain insight into the mechanism driving the instabilities, and to identify simple measures to eliminate the tone. A linear variation of the tone frequency with free-stream velocity (Figure 6) gives indication that the observed tones are driven by the shear-layer instabilities rather than resonance phenomena within the slat volume. Therefore, a streamwise hole dimension and the boundary-layer thickness are considered the dominating length scales. Good agreement is found with the predicted frequencies using Rossiter's⁶ equation for flows over rectangular cavities. The equation is given by

$$\frac{fL_{eff}}{U} = \frac{m - \zeta}{M + \frac{1}{\kappa}}$$

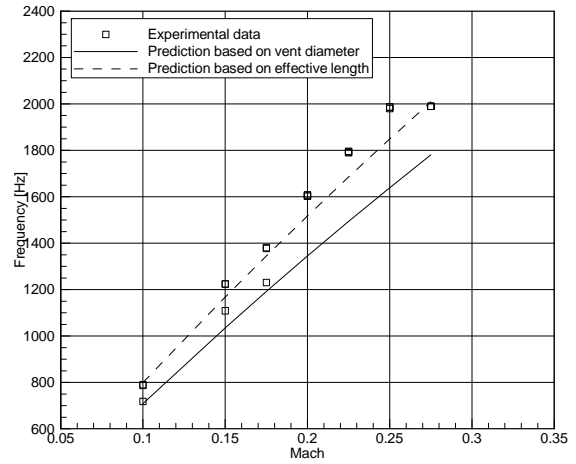


Figure 6. Variation of dominant tone frequency for the baseline vent geometry (D=0.774in) with Mach number. Prediction based on Rossiter's equation using the vent diameter as well as an equivalent effective streamwise length.

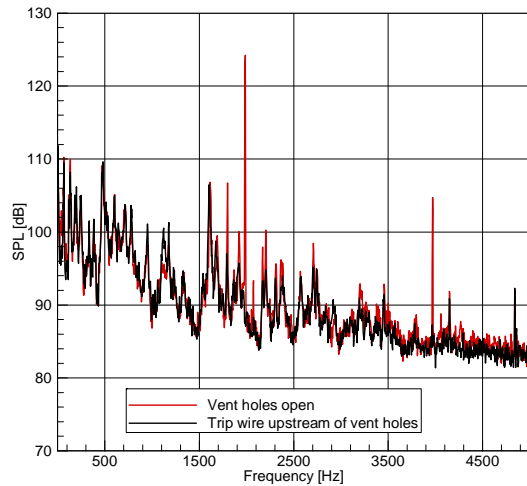


Figure 7. Trip wire installed upstream of the anti-icing vents (M=0.25)

where m is the mode number, M is the Mach number, ζ is an empirical constant accounting for phase lags at impingement, and κ is the average phase speed of the vortical disturbances. Here we use the standard values for the empirical constants: $\kappa=0.57$ and $\zeta=0.25$. The effective streamwise length L_{eff} was calculated based on an equivalent streamwise length for a square vent hole of the same area so that $L_{eff} = \sqrt{\pi D}/2$. This provided a better match to the prediction and is used throughout this study.

Cavity resonance with respect to its depth occurs when the maximum cavity dimension is of the order of a quarter wavelength. The resonance frequency is given by

$$f = \frac{nc}{4H},$$

where n is the mode number, c is the speed of sound and H is the cavity depth. For a circular orifice in an infinite baffle this would yield a fundamental mode at 365Hz if an additional end correction is assumed. A closer examination of the spectra shown in Figure 5 does not show significant tones in this frequency region. The amplitude of the tones remains unchanged if the vents are taped and interactions between the slat volume and the orifice shear layer appear negligible or at least secondary.

A small trip wire is installed three trip wire diameters upstream of the cavity leading edge in analogy to the often deployed small fences or rods upstream of cavities bays as an effective and simple method to eliminate cavity tones (Tramel et al⁹). The effectiveness of this measure is clearly shown in Figure 7 with the cavity tone being removed. The tone was absent over a wide range of Mach numbers showing the upstream implementation of flow-disturbance devices or passive spoilers is a potential solution. Upstream passive devices thicken the boundary layer and move the shear-layer reattachment point beyond the cavity downstream edge. However, an additional drag penalty is paid and the extra manufacturing steps and recurring costs for installation make this a very unattractive option. The potential use of active control scenarios, such as micro-jet blowing (Sarno and Franke¹⁰) or the utilization of piezo-electric elements (Kikuchi and Fukunishi¹¹) would lead to further complications. This limits the design options to variations of the vent-opening shape while keeping the overall venting area constant.

C. Modified vent-hole results

Subsequent tests are carried out in the BRAIT using the same slat model, with only the skin altered to accommodate a replaceable plate. Five additional vent openings were designed with the constraints of maintaining an equal total outflow area, the avoidance of stress concentrations and ease of manufacturing. These hole patterns are shown in Figure 8, along with the baseline hole pattern.

There is, in general, good agreement between the data sets from the two wind tunnels and the variation of the frequency with freestream velocity is approximately linear. The data scatter is of the order of 10dB. The tone emergence relative to the background noise level is in both test phases very significant. It may be possible that some of the differences in the tone amplitudes are due to slight changes in the approaching boundary layer characteristics. As discussed earlier it was difficult to assess the boundary layer state, whether it was laminar or turbulent. However, a small groove was

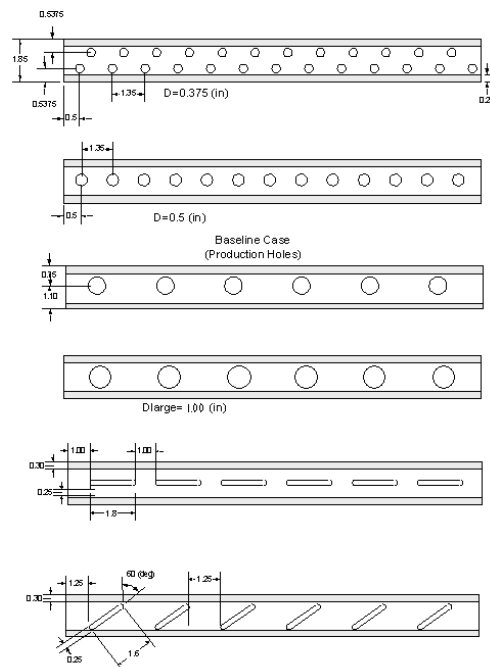


Figure 8. Circular and rectangular vent designs.

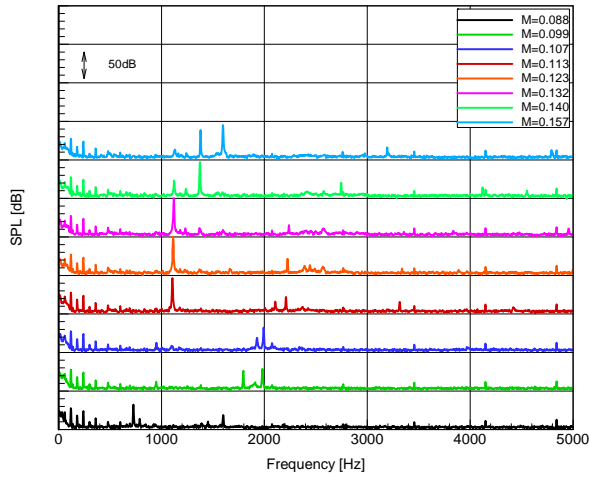


Figure 9. Spectral variation with increase in Mach number for the baseline (0.774") vent geometry. Low Mach number range.

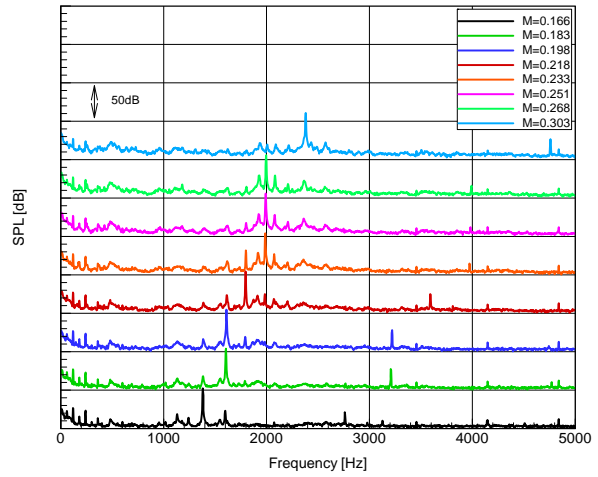


Figure 10 Spectral variation with increase in Mach number for the baseline (0.774") vent geometry. High Mach number range

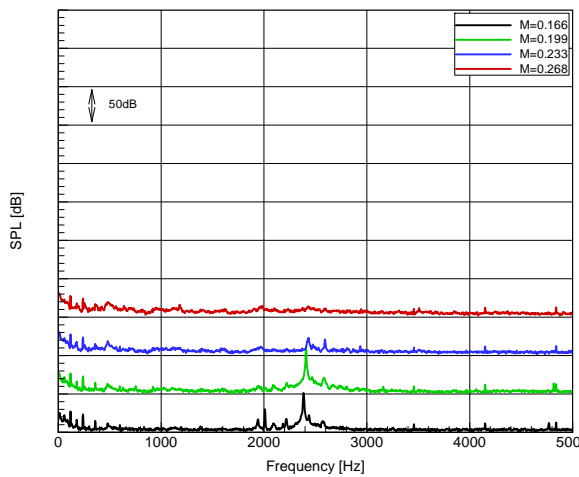


Figure 11. Spectral variation with increase in Mach number for the 0.50" hole geometry.

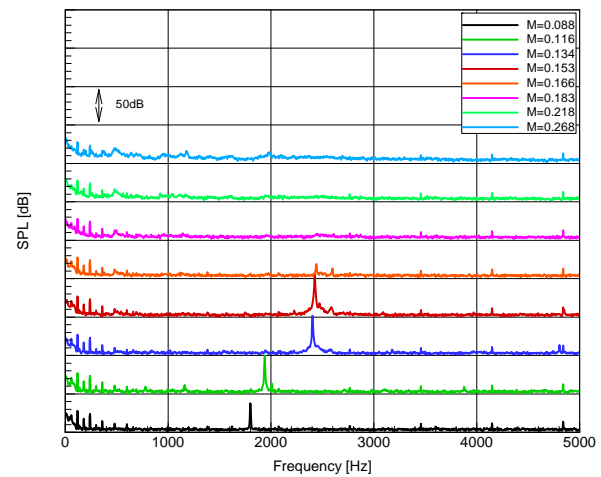


Figure 12. Spectral variation with increase in Mach number for the baseline (0.375") hole geometry.

introduced by utilizing replaceable plates in the BRAIT test and this may have altered the boundary layer type or its characteristics. Unfortunately, no exact measurement of the groove was taken but it may have been of the order of the boundary layer momentum thickness

Figure 9 and Figure 10 illustrate the variation of the energy spectra with Mach number for the baseline vent hole of diameter 0.774in. The results show the presence of tones at all Mach numbers and the occurrence of at least two modes. The second mode is only dominant at two very low Mach numbers and is generally much weaker than the first mode. This higher mode is approximately an integer multiple of the fundamental mode and may be harmonically related. While the tone frequency increases with Mach number this variation is not strictly linear but varies in steps. There is little variation in the tone amplitude when increasing the Mach number from 0.11 to 0.30 and the system loop gain is unity.

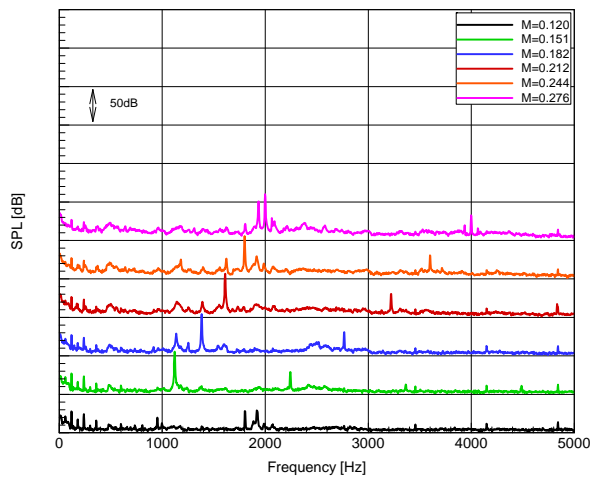


Figure 13. Spectral variation with increase in Mach number for the 1.00" hole geometry.

Results for a reduced vent-hole diameter of 0.5in are shown in Figure 11. Only a limited range of Mach numbers is investigated and strong tones are observed at a Mach number of 0.20 and below. Weak oscillations are detected at $M=0.23$ and results at $M=0.24$ suggest a stable flow bridging the vent opening. Sarohia⁸ suggested that a minimum cavity length exists below which no oscillations would occur for a given flow condition. Based on linear stability theory it can be argued that the overall magnitude of the shear-layer oscillations is the integral of the growth rate over the streamwise distance x . Thus, as the effective length of the vent hole L_{eff} is reduced, so is the level of amplification. Since there are losses associated with the scattering and receptivity stages of the feedback loop, the total gain will eventually drop below unity as L_{eff} is reduced. For a diameter of 0.5in, the cut off occurs near $M\sim 0.2$.

Spectra for an even smaller vent-hole diameter of 0.375in are shown in Figure 12. With the smaller hole diameter, the cut-off Mach number is reduced to $M\sim 0.15$. Although the airplane does not fly at these velocities, it is too close to anticipated flight speeds. A further reduction in the hole diameter would lead to an even greater number of holes, which is considered undesirable as a solution to the vent hole tone. For completeness, a test was conducted with 1in diameter holes to cover a larger range of streamwise vent-hole openings. As expected, the results in Figure 13 show strong oscillations at all Mach numbers.

Two rectangular slots with a 0.25in width were designed where the yaw angle of the major axis to the approach flow was varied from 60 degrees to 90 degrees. As the slot is yawed with respect to the flow, the effective streamwise length of the cavity increases proportional to $1/\sin(\psi)$. Figure 14 shows strong tones in a narrow Mach number range from 0.12 to 0.13 for the slot with the major axis at 60 degrees to the flow. This would be a transient speed range during takeoff and, therefore, not critical for operation. A weak tone may exist at 3500Hz or $St=0.78$ for $M=0.10$ potentially being a second Rossiter⁶ mode. No tones are observed at very low Mach numbers and it seems likely that the inefficient acoustic radiation at those Mach numbers is related to the meager growth that occurs in the shear layer.

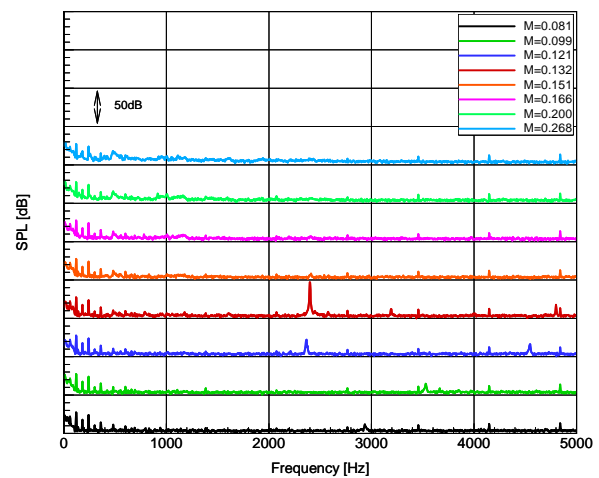


Figure 14. Spectral variation with increase in Mach number for the slot geometry at about 60 degrees yawed with respect to the flow.

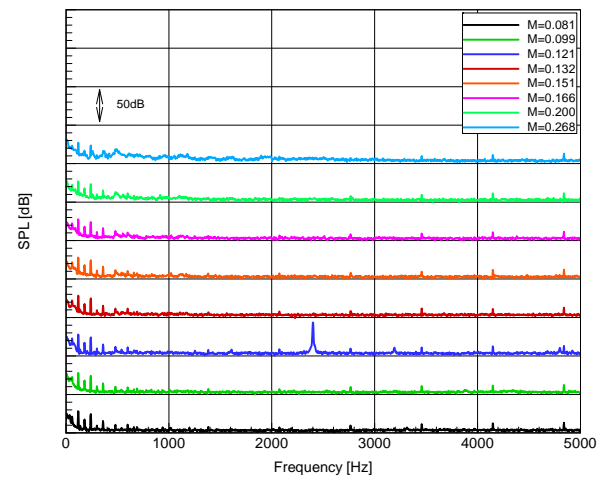


Figure 15. Spectral variation with increase in Mach number for the slot geometry at an approximately normal orientation with respect to the flow.

The normal orientation of the major axis to the flow yields the lowest streamwise dimension of 0.25in for this study. The results in Figure 15 indicate a further drop in minimum Mach number for the onset of oscillations. In this case, only one tone is observed at $M=0.12$. This provided the best overall solution to eliminate the vent tone.

A summary chart of the dominant-mode Strouhal numbers as a function of Mach number is shown in Figure 16. The Mach numbers are corrected for blockage effects. The data set contains all configurations and the Strouhal number is based on the effective streamwise length of the opening. The Strouhal number varies from about 0.4 at $M=0.1$ to 0.35 at $M=0.3$. The collapse of the data is very good with Rossiter's⁶ empirical equation both for the first and second mode.

The basis for the tone cut off with increasing Mach number, observed in Figures 10-15, was not clearly demonstrated. One possible explanation is that the boundary-layer momentum thickness changes due to movement of the transition location. A sudden rise in θ due to transition would result in a reduction in $\sqrt{Re_\theta} L_{eff}/\theta$ and a possible cut off of the tone. Alternatively, there could be a tone cut-off boundary that is crossed when increasing $M\theta/L_{eff}$ where M/L provides a time scale on the mean flow and θ being instrumental in the selection of the natural instability frequency. However, when calculating the $\sqrt{Re_\theta} L_{eff}/\theta$ cut-off limit according to Sarohia⁸ a turbulent boundary layer momentum thickness would have been required to be about twice as large as estimated.

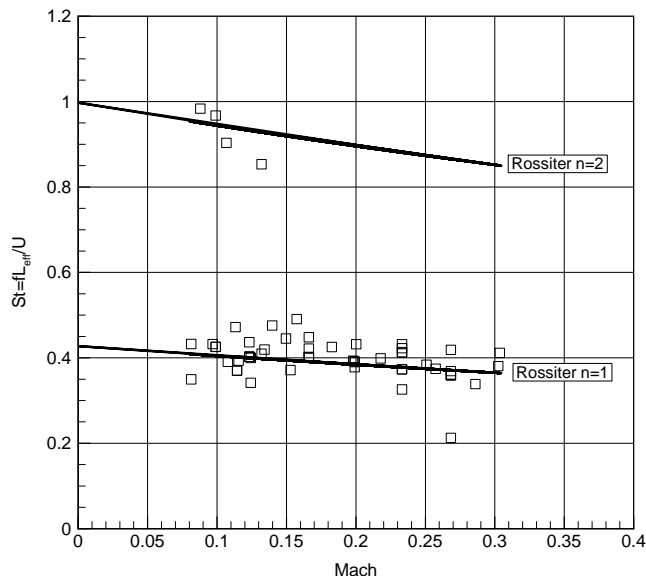


Figure 16. Strouhal number based on the effective stream wise length as a function of Mach number for all test configurations.

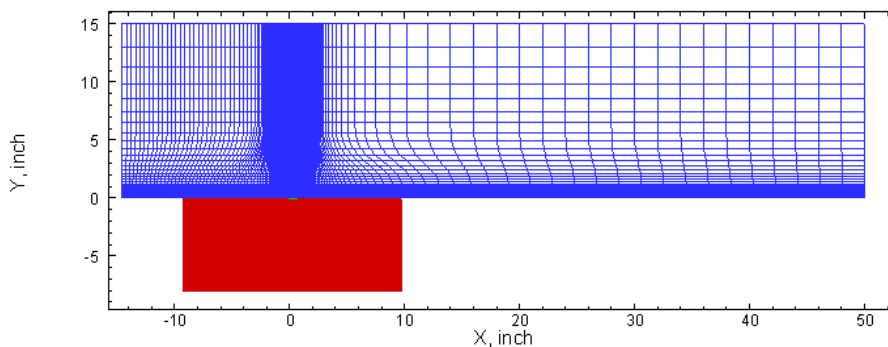


Figure 17. Domain used for numerical-simulation study.

III. Numerical-simulation study

A. Model description

To further examine the mechanism for tone generation, and more specifically tone cutoff, a two-dimensional model problem is developed for investigation using numerical simulations. The basic model geometry is a simplification of a streamwise cut through the slat cavity at a vent-hole location. The model cavity has an 8in deep by 19in long rectangular cross section. The depth is chosen to roughly match the slat-cavity depth measured normal to the surface at the slot location. The cavity slot width is varied from $L=0.2$ to 0.6 in, to match the effective slot width for the various hole geometries. The slot depth is 0.06 in, chosen to match the skin thickness on the slat geometry. The model geometry and the typical grid distribution are shown in Figure 17.

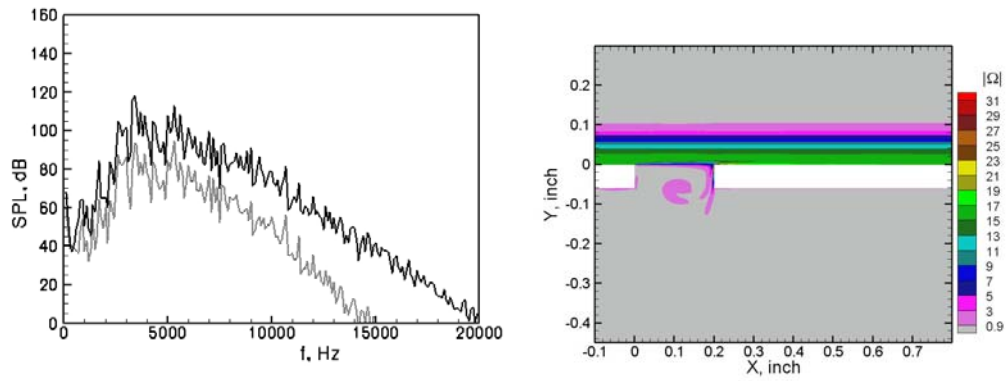


Figure 18. Sound pressure level (100Hz bandwidth) and vorticity contours for case U08, with $L=0.2$, $M=0.2$, $\theta=0.0138$ ($\sqrt{Re_\theta} L/\theta = 621$).

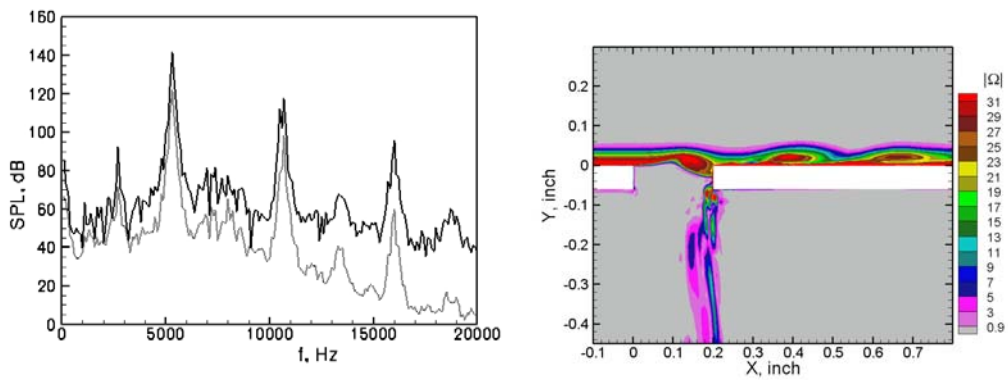


Figure 19. Sound pressure level (100Hz bandwidth) and vorticity contours for case U04, with $L=0.2$, $M=0.2$, $\theta=0.0069$ ($\sqrt{Re_\theta} L/\theta = 878$).

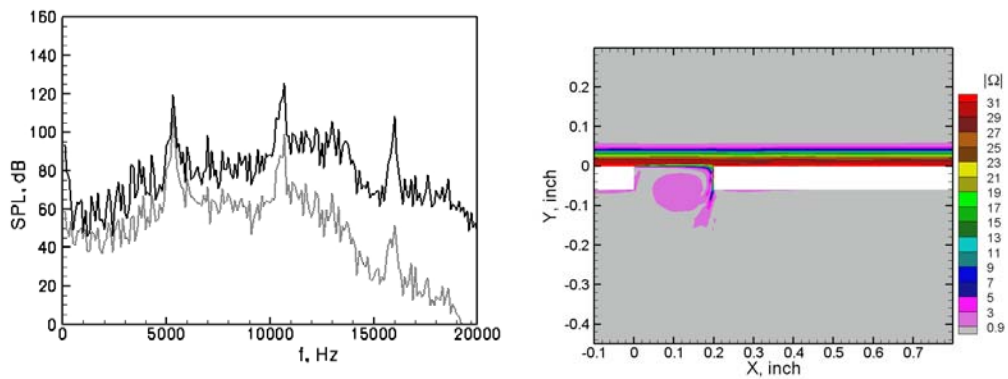


Figure 20. Sound pressure level (100Hz bandwidth) and vorticity contours for case U07, with $L=0.2$, $M=0.5$, $\theta=0.0069$ ($\sqrt{Re_\theta} L/\theta = 878$).

The grid is clustered in the vicinity of the walls and inside the vent-hole and contains about 10^5 cells total. With this grid, a typical cell size in the sensitive area inside the cavity is 5×10^{-2} inch. Preliminary simulations on the coarser grid, with the 4 times larger cell-size did not show any qualitative alteration of the results.

The flow conditions match the typical wind-tunnel conditions, with a nominal unit Reynolds number of 1.60×10^6 per foot. The Mach number ranges from $M=0.2$ to $M=0.5$, based on free-stream conditions. The boundary layer thickness estimates, as discussed above, are used to establish the range of momentum thicknesses used in the calculations. The local Reynolds number, based on the momentum thickness at the separation point, varies from $Re_\theta=306$ to $Re_\theta=1835$ in the simulations.

The time-accurate numerical code is based on Roe's flux-difference splitting method, with the inviscid fluxes approximated using 5th order upwind-biased scheme and the viscous terms approximated using 2nd order central differences (see also ¹²⁻¹⁴). Time-derivatives are approximated with 2nd-order backward differences (three-layer scheme) with dual time-stepping in order to converge sub-iterations at every physical time-step. At each sub-iteration, the resulting finite-difference equations are solved by Gauss-Seidel relaxation by lines. The number of sub-iterations at a time step is within the range from 5 up to 20, which ensures reduction of the maximum residual by 3-4 orders of magnitude. The simulations are conducted using a time step in the range of 0.7×10^{-6} - 3.5×10^{-6} seconds. This resulted in 15-70 time steps per period for the highest tone frequency of about 20kHz. The duration of the runs was long enough to get a statistically mature solution and reliably establish the existence, or non-existence, of tones. Typical run lengths included 100-1500 periods of oscillation associated with the first Rossiter⁶ frequency.

B. Simulation results

Results from the numerical simulations are presented in Figure 18 to Figure 23 for different values of the slot width, momentum thickness, Mach number, and Reynolds number. The sound pressure levels are measured at two locations – one inside the cavity on the lower wall ($x=L/2$, $y=-8.06$), and the other outside the cavity above the vent hole ($x=L/2$, $y=3.0$). The sound pressure levels are based on a 100Hz bandwidth. Vorticity contours near the vent-hole opening are also shown in the figures. The vorticity contours show the development of instabilities in the free shear layer, and the resultant interaction of the concentrated vorticity with the downstream lip of the cavity.

Figure 18 shows the results for a narrow slot opening with a relatively-thick incoming boundary layer. The slot-width parameter for this case is $\sqrt{Re_\theta} L/\theta = 621$. This is below the critical value of $\sqrt{Re_\theta} L/\theta \sim 800$, which Sarohia⁸ found to be necessary for the generation of tones (Rowley et al³). The spectrum shows that no tones are generated, in agreement with the empirical criteria. The vorticity plot shows that the shear layer does not significantly amplify any temporal perturbations.

Figure 19 shows the effect of reducing the incoming momentum thickness. In this case, the parameter $\sqrt{Re_\theta} L/\theta = 878$ is above the critical value, and tones are observed in the spectrum. The shear layer amplifies a dominant mode with a wavelength close to the slot width. The peak frequency corresponds to a Strouhal number of $St=0.39$, which is close to the predicted Rossiter⁶ frequency of $St_1=0.38$. Figure 20 shows the effect of increasing the Mach number. The tone levels are diminished, but the peak-level frequency $St=0.31$ still closely matches the Rossiter⁶ frequency $St_1=0.33$. There is also an increase in the broadband noise level. The shear layer does not show a strongly developed instability

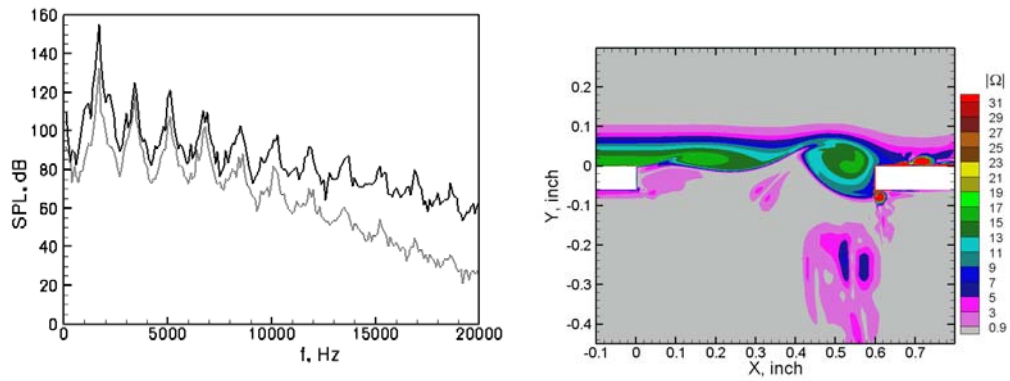


Figure 21. Sound pressure level (100Hz bandwidth) and vorticity contours for case U11, with $L=0.6$, $M=0.2$, $\theta=0.0138$ ($\sqrt{Re_\theta} L/\theta = 1863$).

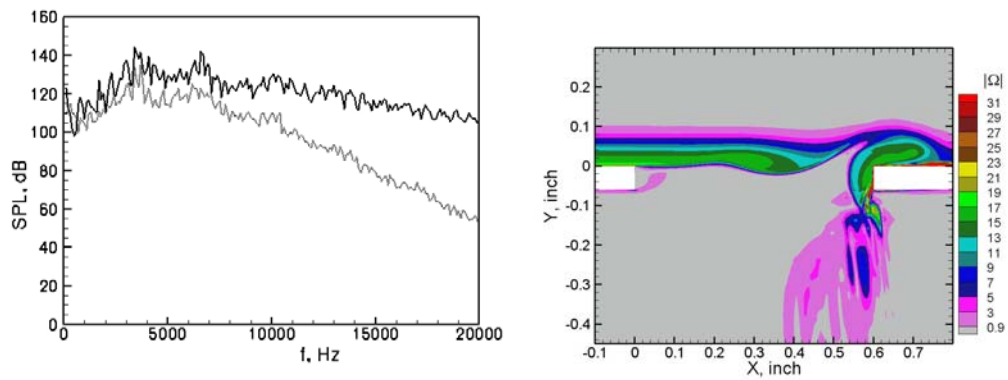


Figure 22. Sound pressure level (100Hz bandwidth) and vorticity contours for case U12, with $L=0.6$, $M=0.4$, $\theta=0.0138$ ($\sqrt{Re_\theta} L/\theta = 1863$).

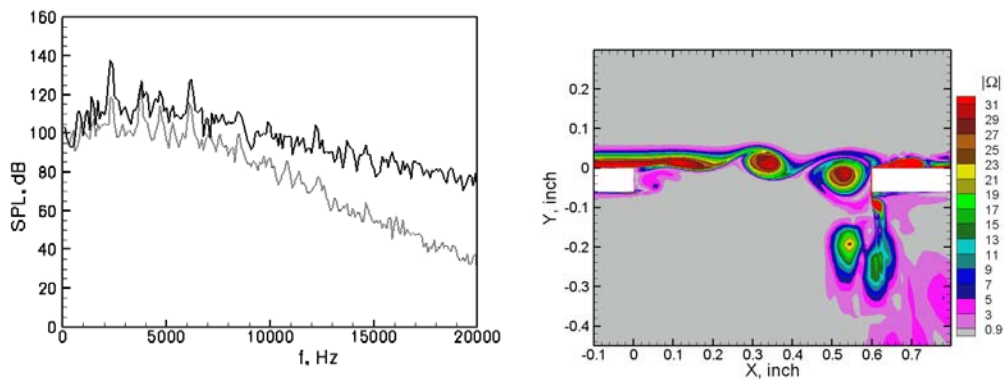


Figure 23. Sound pressure level (100Hz bandwidth) and vorticity contours for case U03, with $L=0.6$, $M=0.2$, $\theta=0.0069$ ($\sqrt{Re_\theta} L/\theta = 2631$).

The results for a larger vent opening are given in Figure 21 except for the cavity slot width L , these are the same flow conditions as in Figure 18. The larger slot width leads to a significant increase in $\sqrt{Re_0} L/\theta$ to 1863. The spectrum shows a very strong tone at $St=0.37$, in close agreement with the Rossiter⁶ frequency $St_1=0.38$. The amplification of the instability is clearly observed in the vorticity contours. The effect of increasing the Mach number is shown in Figure 22. The vorticity plot shows the amplification of instabilities, but no tones are present in the spectrum. However, the broadband noise levels are elevated relative to the lower Mach number case of Figure 21.

Again, comparing to the results of Figure 21, the effect of reducing the momentum thickness is shown in Figure 23. The tone levels are decreased and the broadband level is increased. The dominant tone occurs at $St=0.51$, which is not close to the Rossiter⁶ frequency $St_1=0.38$. Here the slot width is several times greater than the dominant instability wavelength.

Key parameters and results for the different simulation cases are summarized in Figure 24. The blue dashed line shows the critical value for tone generation, $\sqrt{Re_0} L/\theta \sim 800$, based on the results of Sarohia⁸. The two cases below this line do not show tones. For $\sqrt{Re_0} L/\theta = 878$, tones are observed at $M=0.2$ and also at $M=0.5$. At $\sqrt{Re_0} L/\theta = 1863$, tones are observed at $M=0.2$, but not at the higher Mach number, $M=0.4$. For $\sqrt{Re_0} L/\theta = 2631$, tones are observed, but they do not correspond to the Rossiter frequencies.

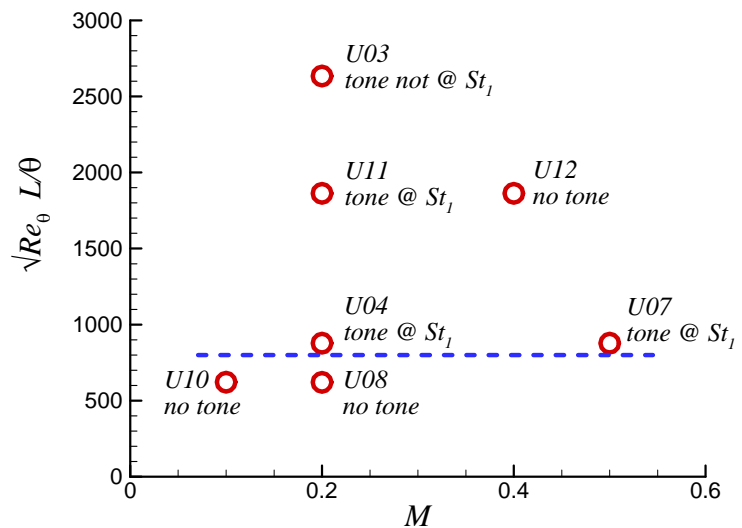


Figure 24. Flow conditions for numerical-simulation cases.

IV. Conclusions

The flow over circular and rectangular vents is studied experimentally and numerically at low subsonic speeds. The wind-tunnel experiments utilize a full-scale 4ft section of a 777 slat to replicate the vent tones observed during flight test. The variation of free stream velocity and vent geometry suggest streamwise flow oscillation similar to the classical cavity case. A good collapse of the data is found by using an effective streamwise dimension for calculating the Strouhal number. A comparison with Rossiter's⁶ prediction for rectangular cavities is excellent and a Strouhal number of about 0.4 is obtained at Mach numbers from 0.1 to 0.3.

Flow over vent holes with sufficiently small streamwise dimension does not resonate at Mach numbers of interest. This resulted in an optimized vent design using rectangular slots with small streamwise extent and was successfully implemented on the recent 777-300ER. The experimental measurements do not provide sufficient detail to definitively define the tone cut-off boundaries as no detailed boundary layer measurements were taken.

Numerical studies complemented the work by investigating the influence of the approaching boundary layer on the tone cut-on and cut-off criteria or different vent lengths. The numerical results are in good agreement with the experimental data and show the shear-layer roll-up characteristics relative to the acoustic spectral content. The numerical results show tone cut on with increasing L/θ for a fixed Mach number, consistent with earlier studies on simple cavities. The numerical simulations also show evidence of tone cut off with increasing Mach number at higher values of L/θ . At the largest values of $\sqrt{Re_0} L/\theta$ considered, the shear-layer mode does not appear to be operative.

References

- ¹Rockwell, D. and Naudascher, E. "Self-sustaining oscillations of impinging free shear layers", *Ann. Rev. Fl. Mech.*, 11:67-94, 1979
- ²Gharib, M. and Roshko A., "The effect of flow oscillations on cavity drag", *J Fluid Mechanics*, Vol 177, 1987, pp501-530
- ³Rowley, C., Colonius, T. and Basu, A. "On self-sustaining oscillations in two-dimensional compressible flow over rectangular cavities", *J. Fluid Mech.*, 2002, vol 455, pp315-346
- ⁴Blake, W. and Powell, A. "The development of contemporary views of flow-tone generation, *Recent Adv. Aeroacoustics*, 247-345, 1986
- ⁵Colonius, T. "An overview of simulation, modeling, and active control of flow/acoustic resonance in open cavities", *AIAA Paper 2001-0076*
- ⁶Rossiter, J. "Wind-tunnel experiments on the flow over rectangular cavities at subsonic and transonic speeds", *ARCRM*, 3438, 1964
- ⁷Kerschen, E. and Tumin, E. "A theoretical model of cavity acoustic resonances based on edge scattering processes", *AIAA-paper 2003-0175*, 2003
- ⁸Sarohia, V. "Experimental investigation of oscillations in flows over shallow cavities", *AIAA J.*, 15, 984-991, 1977
- ⁹Tramel R., S. Rock and J. Ellis, *Digital Fusion*, Huntsville, AL; D. Sharpes, U.S. Air Force, Kirtland AFB, NM *AIAA-2005-2800*
- ¹⁰Sarno, R. and Franke, M. "Suppression of flow-induced pressure oscillations in cavities", *Journal of Aircraft*, 31(1):90-96, 1994
- ¹¹Kikuchi, S. and Fukunishi, Y. "Active flow control technique using piezo-film actuators applied to the sound generation by a cavity". *ASME FEDSM99-7232*, 1999
- ¹²Strelets, M. "Detached-Eddy Simulation of Massively Separated Flows", *AIAA Paper 2001-0879*
- ¹³Shur, M., Strelets, M., Travin, A. "High-Order Implicit Multi-Block Navier-Stokes Code: Ten-Year Experience of Application to RANS/DES/LES/DNS of Turbulence." In: *7th Symposium on Overset Grids & Solution Technology*, October 5-7, 2004, Huntington Beach, CA, USA
- ¹⁴Shur, M., Spalart, P., Strelets, M. "Noise Prediction for Increasingly Complex Jets. Part I, Methods and tests." *Int. J. Aeroacoustics* 4, 3-4, 213-266.